Draft version February 14, 2017
Preprint typeset using LaTeX style emulateapj v. 12/16/11

PROXIMA CENTAURI B WATER LOSS

Rodrigo Luger

1. INTRO

We perform a suite of Markov Chain Monte Carlo (MCMC) runs to obtain constraints on the present-day water content of Proxima Centauri b using the Python code package `emcee` (Foreman-Mackey et al. 2013). MCMC allows one to sample from multi-dimensional probability distributions that are difficult or impossible to obtain directly, which is the case for the ensemble of parameters that control the evolution of the planet surface water content in `VPLANET`. In this section, we develop a framework for inferring the probability distributions of these parameters conditioned on empirical data and our understanding of the physical processes at play.

The input parameters to our model make up the state vector $\mathbf{x}$:

$$\mathbf{x} = \{f_{\rm sat}, t_{\rm sat}, \beta_{\rm xuv}, M_\star, t_\star, a, m\}, \tag{1}$$

corresponding, respectively, to the stellar mass, the XUV saturation fraction, the XUV saturation timescale, the XUV power law exponent, the stellar age, the semi-major axis of the planet, and the mass of the planet. Given a value of $\mathbf{x}$, `VPLANET` computes the evolution of the system from time $t = 0$ to $t = t_\star$, yielding the output vector $\mathbf{y}$:

$$\mathbf{y}(\mathbf{x}) = \{L_\star, L_{\rm xuv}, t_{\rm RG}, m_{\rm H}, m_{\rm H_2O}, m_{\rm O_2}\}, \tag{2}$$

corresponding, respectively, to the stellar luminosity, the stellar XUV luminosity, the duration of the runaway greenhouse phase, the mass of the planet's hydrogen envelope, the mass of water remaining on its surface, and the mass of oxygen retained in either the atmosphere or the surface/mantle, all of which are evaluated at $t = t_\star$ (i.e., the present day). Additional parameters that control the evolution of the planet (initial water content, XUV absorption efficiency, etc.) are held fixed in individual runs; see below.

Our goal in this section is to derive posterior distributions for $\mathbf{y}$ (and in particular for $m_{\rm H_2O}$) given prior information on both $\mathbf{x}$ and $\mathbf{y}$. Some parameters—such as the present-day stellar luminosity—are well-constrained, while others are less well-known and will thus be informed primarily by our choice of prior. This is the case for the XUV saturation fraction, saturation timescale, and power law exponent, which have been studied in detail for solar-like stars (Ribas et al. 2005) but are poorly constrained for M dwarfs. More info on them here... We therefore use flat-log priors for the saturation fraction and timescale, enforcing $-5 \leq \log(f_{\rm sat}) \leq -2$ and $-0.3 \leq \log(t_{\rm sat}/{\rm Gyr}) \leq 1$. We use a Gaussian prior for the XUV power law exponent, with a mean of 1.23, the value derived by (Ribas et al. 2005) for solar-like stars: $\beta_{\rm xuv} \sim \mathcal{N}(-1.23, 0.1)$. We choose an ad hoc standard deviation $\sigma = 0.1$ because...

We also use a flat prior for the stellar mass ($0.1 \leq M_\star/{\rm M}_\oplus \leq 0.15$). Although stronger constraints on the stellar mass exist (cite), these are derived indirectly from mass-luminosity relations; we thus enforce a prior on the present-day luminosity to constrain the value of $M_\star$ via our stellar evolution model (see below). We enforce a Gaussian prior on the stellar age $t_\star \sim \mathcal{N}(4.8, 1.4^2)$ Gyr based on the constraints discussed in §(cite).

Our prior on the semi-major axis a is a combination of a Gaussian prior on the orbital period, $P \sim \mathcal{N}(11.186, 0.002^2)$ days (Anglada-Escudé et al. 2016), and the stellar mass prior. Finally, our prior on the planet mass m combines the empirical minimum mass distribution, $m \sin i \sim \mathcal{N}(1.27, 0.18^2)$ ${\rm M}_\oplus$ (Anglada-Escudé et al. 2016), and the a priori inclination distribution for randomly aligned orbits, $\sin i \sim \mathcal{U}(0, 1)$, where $\mathcal{U}$ is a uniform distribution (e.g., Luger et al. 2016).

We further condition our model on measured values of the stellar luminosity $L_\star$ and stellar XUV luminosity $L_{\rm xuv}$. We take $L_\star \sim \mathcal{N}(1.65, 0.15) \times 10^{-3}$ ${\rm L}_\odot$ (Demory et al. 2009) and $\log L_{\rm xuv} \sim \mathcal{N}(-6.36, 0.3^2)$. We base the latter on Ribas et al. (2016), who compiled a comprehensive list of measurements of the emission of Proxima Centauri in the wavelength range 0.6–118 nm. Summing the fluxes over this range and neglecting the contribution of flares, we obtain an XUV flux at Proxima Centauri b $F_{\rm xuv} \approx 252$ erg cm^{-2} s^{-1}, corresponding to $\log L_{\rm xuv} = -6.36$ for $a = 0.0485$ AU. Given the lack of uncertainties for many of the values compiled in Ribas et al. (2016) and the fact that some of those estimates are model extrapolations, it is difficult to establish a reliable error estimate for this value. We make the ad hoc but conservative choice $\sigma = 0.3$ dex, noting that the three measurements that inform the X-ray luminosity of the star in Ribas et al. (2016) (which dominates its XUV emission) have a spread corresponding to $\sigma = 0.2$ dex. However, more rigorous constraints on the XUV emission of Proxima Cen with reliable uncertainties are direly needed to obtain more reliable estimates of water loss from Proxima Cen b.

Given these constraints, we wish to find the posterior distribution of each of the parameters in Equations (1) and (2). We thus define our likelihood function $\mathcal{L}$ for a given state vector $\mathbf{x}$ as

$$\ln \mathcal{L}(\mathbf{x}) = -\frac{1}{2}\left[\frac{(L_\star(\mathbf{x}) - L_\star)^2}{\sigma_{L_\star}^2} - \frac{(L_{\rm xuv}(\mathbf{x}) - L_{\rm xuv})^2}{\sigma_{L_{\rm xuv}}^2}\right] + \ln {\rm Prior}(\mathbf{x}) + C, \tag{3}$$

where $L_\star(\mathbf{x})$ and $L_{\rm xuv}(\mathbf{x})$ are, respectively, the model predictions for the present-day stellar luminosity and stellar XUV luminosity given the state vector $\mathbf{x}$, $L_\star$ and $L_{\rm xuv}$ are their respective observed values, and $\sigma_{L_\star}^2$ and $\sigma_{L_{\rm xuv}}^2$ are the uncertainties on those observations. The $\ln {\rm Prior}(\mathbf{x})$ term is the prior probability and C is an arbitrary normalization constant. Expressed in this form, the

observed values of $L_\star$ and $L_{\rm xuv}$ are our "data," while the constraints on the other parameters are "priors," though the distinction is purely semantic.

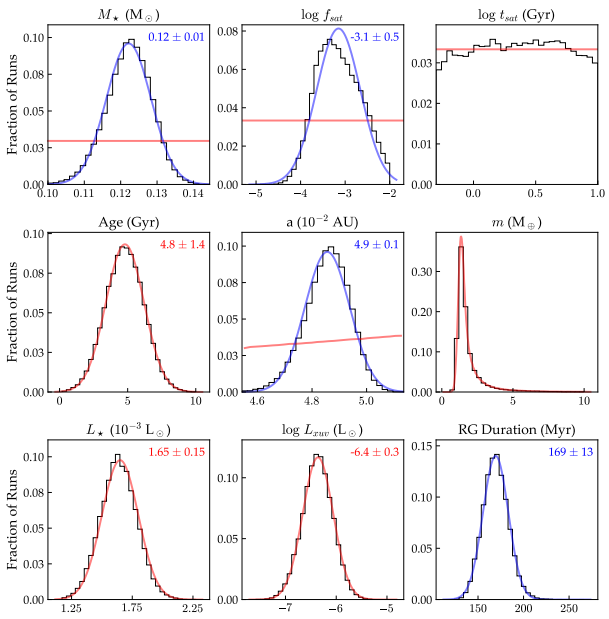

FIG. 1.— Posterior distributions for the various stellar parameters used in the model. The first eight parameters are model inputs, with their corresponding priors shown in red. The combination of these priors and the physical models in `VPLANET` constrain the stellar and planetary parameters shown in this section. Blue curves show Gaussian fits to the posterior distributions, with the mean and standard deviation indicated at the top right. The last panel shows the duration of the runaway greenhouse phase for Proxima Centauri b, one of the model outputs, which we find to be 169 ± 13 Myr.

Given this likelihood function, we use MCMC to obtain the posterior probability distributions for each of the parameters of interest. We draw each of the $\mathbf{x}$ from their respective prior distributions and run 40 parallel chains of 5,000 steps each, discarding the first 500 steps as burn-in. The posterior distributions for the stellar mass, saturation fraction, saturation timescale, age, semi-major axis, planet mass, present-day stellar luminosity, present-day stellar XUV luminosity, and duration of the runaway greenhouse are shown in Figure 1 as the black histograms. The red curves indicate our priors/data, and the purple curve is a Gaussian fit to the runaway greenhouse duration posterior, yielding $t_{\rm RG} = 169 \pm 13$ Myr.

By construction, the planet mass, stellar age, present-day stellar luminosity, and present-day stellar XUV luminosity posteriors reflect their prior distributions. As mentioned above, the stellar mass posterior is entirely informed by the luminosity posterior via the Spada et al. (2013) stellar evolution tracks. The stellar mass in turn constrains the semi-major axis (via the prior on the period and Kepler's laws). The XUV saturation fraction

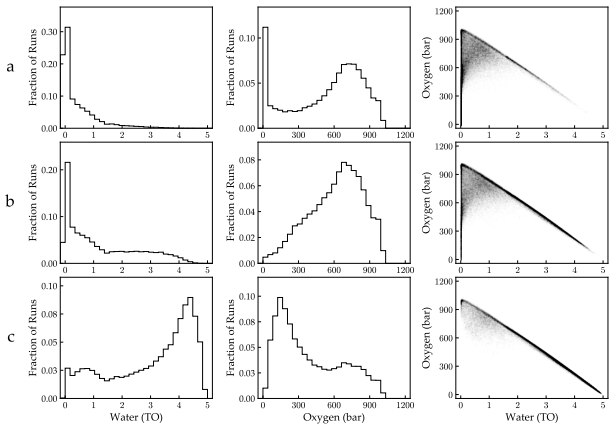

FIG. 2.— Planet posteriors (epsilon).

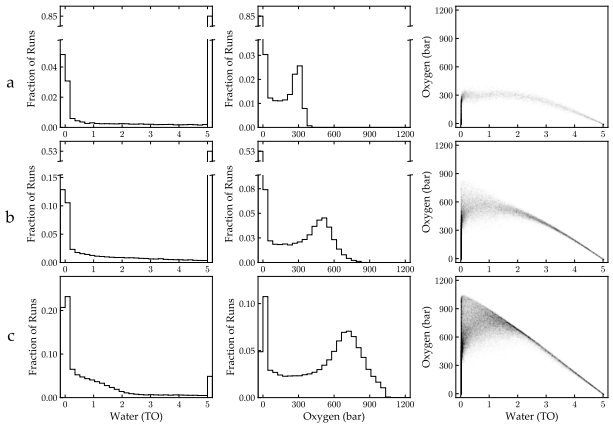

FIG. 3.— Planet posteriors (hydrogen).

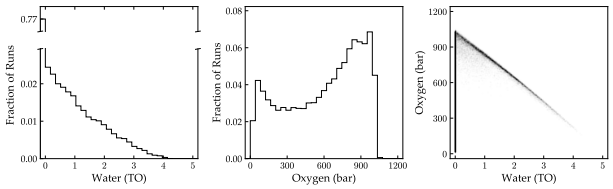

FIG. 4.— Planet posteriors (magma).

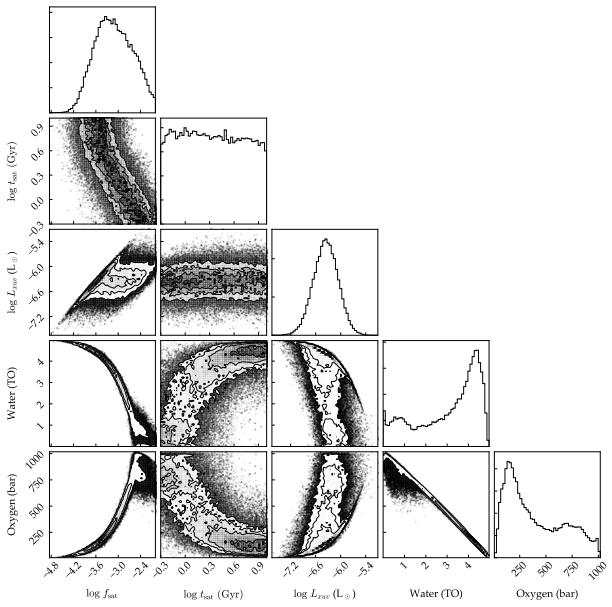

FIG. 5.— Correlations.

REFERENCES

Anglada-Escudé, G., Amado, P. J., Barnes, J., Berdiñas, Z. M., Butler, R. P., Coleman, G. A. L., de La Cueva, I., Dreizler, S., Endl, M., Giesers, B., Jeffers, S. V., Jenkins, J. S., Jones, H. R. A., Kiraga, M., Kürster, M., López-González, M. J., Marvin, C. J., Morales, N., Morin, J., Nelson, R. P., Ortiz, J. L., Ofir, A., Paardekooper, S.-J., Reiners, A., Rodríguez, E., Rodríguez-López, C., Sarmiento, L. F., Strachan, J. P., Tsapras, Y., Tuomi, M., & Zechmeister, M. 2016, Nature, 536, 437

Demory, B.-O., Ségransan, D., Forveille, T., Queloz, D., Beuzit, J.-L., Delfosse, X., di Folco, E., Kervella, P., Le Bouquin, J.-B., Perrier, C., Benisty, M., Duvert, G., Hofmann, K.-H., Lopez, B., & Petrov, R. 2009, A&A, 505, 205

Foreman-Mackey, D., Hogg, D. W., Lang, D., & Goodman, J. 2013, PASP, 125, 306

Luger, R., Lustig-Yaeger, J., Fleming, D. P., Tilley, M. A., Agol, E., Meadows, V. S., Deitrick, R., & Barnes, R. 2016, ArXiv e-prints

Ribas, I., Bolmont, E., Selsis, F., Reiners, A., Leconte, J., Raymond, S. N., Engle, S. G., Guinan, E. F., Morin, J., Turbet, M., Forget, F., & Anglada-Escudé, G. 2016, A&A, 596, A111

Ribas, I., Guinan, E. F., Güdel, M., & Audard, M. 2005, Astrophys. J., 622, 680

Spada, F., Demarque, P., Kim, Y.-C., & Sills, A. 2013, ApJ, 776, 87